JOURNAL OF SPACECRAFT AND ROCKETS
Vol. 41, No. 6, November–December 2004

Attitude Stability of Blunt-Body Capsules in Hypersonic Rarefied Regime

Kazuhisa Fujita,* Yoshifumi Inatani,† and Kojyu Hiraki‡
Institute of Space and Astronautical Science, Kanagawa 229-8510, Japan

To assess the attitude stability of blunt-body reentry capsules in the hypersonic rarefied flight regime, a systematic numerical procedure has been developed and applied practically to the asteroid sample return capsule. The low-density flows around the capsule are solved by the direct simulation Monte Carlo (DSMC) method in the three-dimensional geometry to determine the low-density aerodynamic coefficients. The overall aerodynamic coefficients are defined by an empirical bridging formula from the results of the DSMC analysis and the continuum coefficients obtained by the modified Newtonian method. By the use of these overall coefficients, the six-degree-of-freedom dynamics of the capsule is analyzed along the reentry trajectory. It is shown that the static instability about the pitching axis occurs in the low-density environments when the center of gravity is located in the rear part of the capsule. However, the pitching motion is found to be stabilized safely by initiation of the spin around the capsule axis at appropriate frequencies.

Introduction

HYPERSONIC vehicles reentering the atmospheric planets experience a wide range of gas densities, from the rarefied to dense gas environments, along the flight trajectory. As the gas density decreases, rarefaction of flows around the vehicle begins to have a considerable influence on the aerodynamic characteristics of the vehicle. In particular, it is important to estimate qualitatively such influences on the pitching moment because the pitching moment acting on the vehicle plays a significant role in stabilizing the attitude of the vehicle. Blunt-body reentry capsules that are frequently used in recent missions are designed to maintain static and dynamic stability in the hypersonic flight environments when the flow around the capsule can be regarded as continuous. However, the stability of such capsules is, in general, degraded as the flow becomes rarefied. To take the Stardust sample return capsule of NASA as an example,[1] the pitching moment coefficient becomes positive for positive angles of attack as the Knudsen number based on the capsule diameter increases above 0.1. That is, the capsule is expected to become statically unstable about the pitching motion in the early phase of reentry.

A similar instability due to rarefaction of the flow is considered to occur to the sample return capsule of the third Mu Space Engineering Spacecraft (MUSES-C) asteroid explorer, launched by the Institute of Space and Astronautical Science,[2] because it has a blunt-body form similar to the Stardust capsule (Fig. 1). Unless a large angle of attack induced by such instabilities at high altitudes can be damped before the aerodynamic heating increases at lower altitudes, the capsule might be damaged due to an anomalous heating distribution to the capsule surface. To cope with these problems, a numerical procedure has been developed and applied practically to the assessment of the attitude stability of the MUSES-C capsule in the rarefied gas environments, from the free-molecular to transitional flight regimes. The procedure and its application are discussed in this paper.

The nominal aerodynamic coefficients of the MUSES-C capsule have been summarized in the MUSES-C aerodynamic database by Hiraki and Inatani[3] for the entire flight environments encountered by the capsule. However, the hypersonic aerodynamic coefficients are recomputed in this study to examine the influence of uncertainties in gasdynamic processes on the aerodynamic characteristics of the capsule and estimate the accuracy of the aerodynamic coefficients. In this paper the low-density aerodynamic coefficients are computed by the direct simulation Monte Carlo (DSMC) method, whereas the continuum coefficients are calculated by the modified Newtonian method. The overall coefficients are determined by an empirical bridging formula that takes both the low-density and continuum coefficients into account. Finally, the pitching stability of the capsule is assessed by a six-degree-of-freedom analysis of the capsule dynamics along the flight trajectory by the use of the overall coefficients.

Low-Density Aerodynamic Coefficients

Free-Molecular Flows

As the limit case of low-density flows, the aerodynamic coefficients in the free-molecular flow are calculated first. Because the reentry velocity of the MUSES-C capsule is as high as 12 km/s, which is much higher than the average thermal velocity of atmospheric gases at altitudes below 200 km (∼700 m/s), molecules hitting against the capsule surface can be assumed to have a unique velocity equal to the flight speed of the capsule. The aerodynamic force acting on the capsule is computed by a geometric analysis, integrating the change in kinetic momentum of molecules through collisions against the capsule surface.

The axial force coefficient C_A, the normal force coefficient C_N, and the pitching moment coefficient C_m are defined by

$$C_{A,N} = F_{A,N}/(\pi/8)\rho V^2 D^2 \tag{1}$$

$$C_m = M/(\pi/8)\rho V^2 D^3 \tag{2}$$

where F_A and F_N are the axial and normal force, respectively; M is the pitching moment around the c.g.; ρ and V are the freestream density and velocity, respectively; and D is the capsule diameter equal to 0.404 m. Molecules are assumed to be scattered on the capsule surface by the Maxwell model with a linear mixture of diffusive and specular reflection. That is, molecules are either reflected by diffusive scattering with a probability of γ, which is the so-called accommodation factor, or by specular reflection. In the

Presented as Paper 2003-3893 at the AIAA 36th Thermophysics Conference, Orlando, FL, 23 June 2003; received 4 July 2003; revision received 5 October 2003; accepted for publication 13 October 2003.

*Research Associate, 3-1-1 Yoshinodai, Sagamihara; kazu@kazudom.eng.isas.jaxa.jp. Member AIAA.
†Professor, 3-1-1 Yoshinodai, Sagamihara. Senior Member AIAA.
‡Research Associate; currently Associate Professor, Faculty of Engineering, Kyushu Institute of Technology, Fukuoka 804-8550, Japan. Member AIAA.

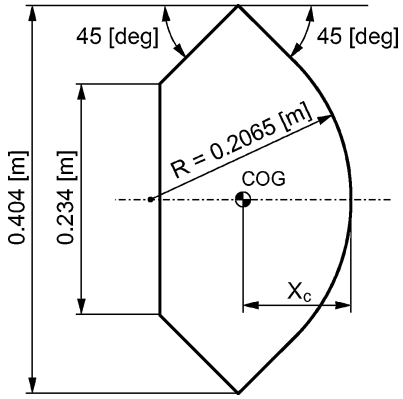

Fig. 1 Schematic of MUSES-C capsule.

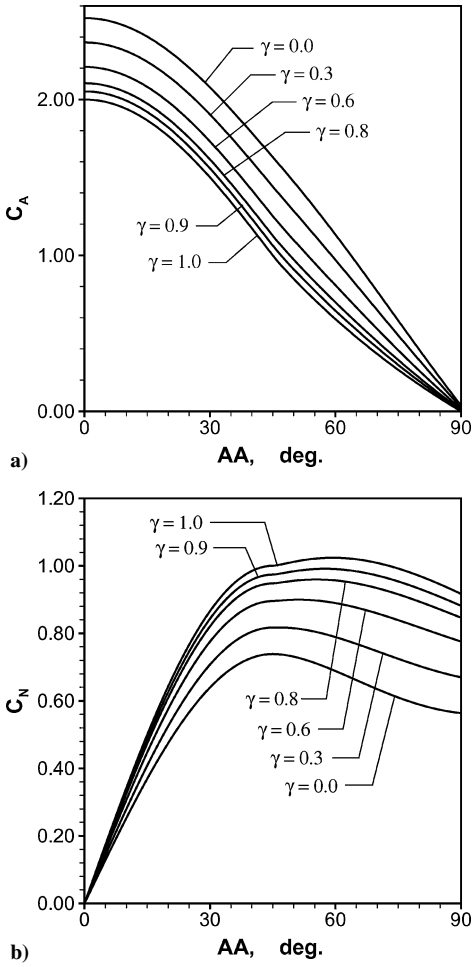

Fig. 2 Free-molecular aerodynamic coefficients: a) axial force coefficient and b) normal force coefficient.

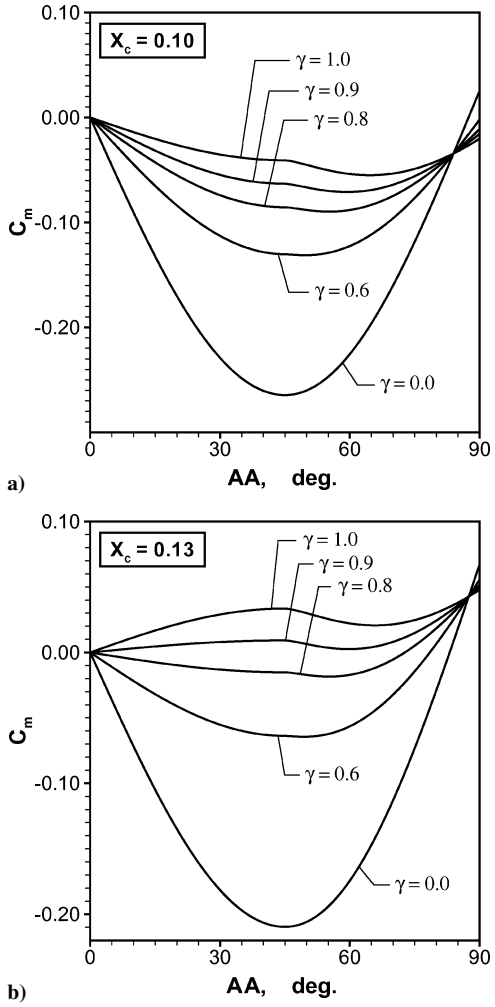

Fig. 3 Free-molecular pitching moment coefficient: a) $X_c = 0.10$ m and b) $X_c = 0.13$ m.

context, of particle scattering, $\gamma = 1$ indicates a fully diffusive surface, and $\gamma = 0$ represents a fully specular surface. Influences of the scattering model on the aerodynamic coefficients are examined by changing γ from 0 to 1.

In diffusive scattering, the aerodynamic coefficients are considered dependent on the temperature of the capsule surface because the reflected molecules are assumed to have thermal velocities corresponding to the surface temperature. However, for the MUSES-C reentry, because the flow velocity is much higher than the thermal velocities at high altitudes, the surface temperature is found to have little influence on the aerodynamic coefficients. For this reason, the free-molecular aerodynamic coefficients given hereafter are calculated by neglecting the thermal velocity in the diffusive scattering.

The axial and normal force coefficients, and the pitching moment coefficients in the free-molecular flow, are plotted against the angle of attack (AOA) in Figs. 2 and 3, respectively. In Figs. 2 and 3, X_c is the distance of the c.g. from the capsule forefront (Fig. 1). The aerodynamic coefficients, especially C_m, are found to be very sensitive to γ. For $X_c = 0.13$ m, as seen in Fig. 3b, the pitching stability becomes degraded as γ increases, and the capsule is unstable for any AOA (<90 deg) for $\gamma \geq 0.9$. The reason for the decrease in the pitching stability along with the increase of γ is an increase of the tangential momentum transferred by molecules to the capsule surface, which increases the pitch-up moment even for positive AOA. I. assess of the attitude stability, it is sufficient to use the most conservative values of the pitching moment coefficient. For this reason, the results calculated with $\gamma = 1.0$ are used as the free-molecular aerodynamic coefficients in the following analysis.

DSMC Model for Rarefied Flows

To calculate the aerodynamic coefficients in the transitional flight regime, low-density flows around the capsule are calculated by the DSMC method in the three-dimensional geometry. The DSMC computer code used in this analysis is RARAC3D (Ref. 4), which is a general-purpose program for analysis of rarefied atmospheric flows with nonequilibrium thermal relaxation and chemical kinetics involved. RARAC3D employs the no-time-counter (NTC) algorithm of Bird for the DSMC calculation[5] and the variable hard

sphere (VHS) model for collision cross sections.[6] Adjusting parameters of the VHS model are determined from the viscosity of a single-species gas for collisions between two molecules of the same species, whereas those for collisions between the different species are determined from the binary diffusion coefficient of the corresponding gas mixture.[7] At high temperatures, the single-species viscosity and the binary diffusion coefficient are calculated with the collision integrals given by Capitelli et al.[8]

The probability of the rotationally inelastic collision is calculated by the Boyd model.[9] Adjusting parameters in this model are determined, so that they can reproduce the rotational collision number of (see Ref. 10) Lordi and Mates[11] in the equilibrium limit. It is often pointed out that this collision number is verified experimentally only at low temperatures below several thousand Kelvin. However, recent studies by Fujita and Abe[12,13] have shown that their validity can be extended to higher temperatures up to 60,000 K. On the other hand, the probability of the vibrationally inelastic collision is determined as a cell-average probability from the vibrational relaxation time determined by Millikan and White with the high-temperature correction introduced by Park.[14] Inelastic collisions involving electronic transitions are neglected because they hardly occur in the rarefied gases under consideration. Redistribution of the molecular internal energy after a collision is calculated by the Borgnakke–Larsen phenomenological model.[15]

In the free-molecular and transitional flows of the MUSES-C reentry under consideration, ionization remains a rare event compared with dissociation of the molecular species. For this reason, and to reduce the computational cost, five air species of N_2, O_2, N, O, and NO are taken into account. Chemical reactions selected for the five air species system are dissociation, recombination, and particle-exchange reactions, which amount to 34 reactions in total, as summarized in Table 1. The probabilities of the dissociative and the particle-exchange collisions are calculated according to Bird's approach,[16] whereas those of the three-body recombination are computed by the Boyd model.[17] These models are adjusted so that the bulk reaction rate asymptotically approaches the macroscopic reaction rate determined by Park[14] in the equilibrium limit.

To make a conservative estimation of the pitching moment coefficient, as in the free-molecular flow analysis, the diffusive scattering on the capsule surface is assumed to be $\gamma = 1$. Because the translational temperature reaches the tens of thousand Kelvin in the shock layer, the velocity of molecules scattered on the capsule surface is much lower than that of molecules hitting against the surface. In such a situation, the capsule surface temperature is only a minor factor to change the aerodynamic coefficient. For this reason, T_w was set uniquely to be 500 K for all of the cases.

RARAC3D employs a multilevel rectangular grid system[18,19] composed of hierarchical rectangular parallelepiped cells with a solution-adaptive strategy. Based on the local Knudsen number criteria (see Ref. 19) a parent cell is divided into eight child cells, each of which can be further divided into eight grandchild cells, and so on. First, the DSMC calculation is started with the initial grid system consisting of the parent cells until flowfield convergence, then the average flowfield is determined with an ensemble average. With this average flowfield, the cell Knudsen number based on the cell length in the x direction (and similarly in the y and z directions), and the local scale lengths of the density and temperature gradient,[19] $\rho/(\partial\rho/\partial x)$ and $T/(\partial T/\partial x)$, respectively, are determined at each cell. The grid system is then reconstructed by division or recombination of hierarchical cells, so that the cell length becomes shorter than the local scale lengths and so that the local Knudsen number becomes larger than unity. The DSMC calculation is continued with this new grid system, and an ensemble average is taken after 5000 steps to determine the average flowfield, from which a new grid system is regenerated. These procedures are continued until we obtain a convergence for the aerodynamic coefficients.

Table 1 Chemical reactions considered

Reactions 1–5	Reaction rate
$N_2 + M^a \leftrightarrow 2N + M$	Ref. 14
$O_2 + M \leftrightarrow 2N + M$	Ref. 14
$N_2 + O \leftrightarrow N + NO$	Ref. 14
$O_2 + N \leftrightarrow O + NO$	Ref. 14
$NO + M \leftrightarrow N + O + M$	Ref. 14

[a]M = N_2, O_2, N, O, or NO.

DSMC Results

The DSMC analysis was performed for four representative flight environments listed in Table 2. The Knudsen number Kn in Table 2 is defined with the capsule diameter 0.404 m as the representative length and the mean free path in the freestream. In addition to these four cases, a collisionless DSMC calculation was made to obtain a free-molecular flow solution, which is expected to coincide with that obtained by the geometric analysis of the free-molecular flow in the preceding section. Selected angles of attack are 0, 10, and 20 deg for each case.

To demonstrate the convergence of the flowfield and the aerodynamic coefficients in the DSMC calculation, Fig. 4 illustrates the variation of the aerodynamic coefficients and the total cell number along with the calculation time step, which was obtained for case C in Table 2 with an AOA of 20 deg. In this case, a distinct trend of the variation is found until the 50,000th time step. The aerodynamic coefficients and the total element number are considered to converge in the subsequent steps because they are distributed with a certain deviation around the final solution determined as an average value. Such a deviation is essentially inevitable in the DSMC method used in this analysis because it originates from the statistical

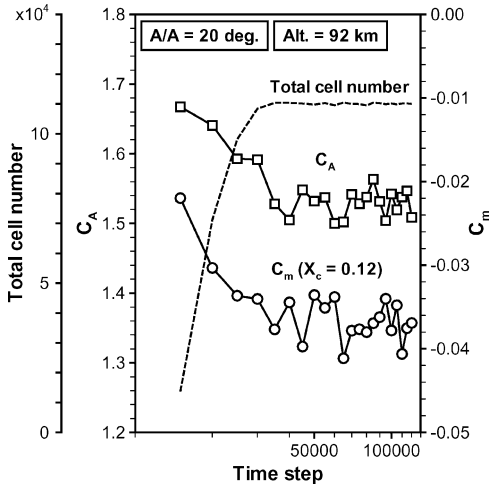

Fig. 4 Variation of aerodynamic coefficients and total cell number (altitude, 92 km and AOA, 20 deg).

Table 2 Flow conditions for DSMC analysis

Case	Altitude, km	Velocity, km/s	Temperature, K	Pressure, Pa	Kn	Mole concentration N_2	O_2	O
A	120	12.26	394.7	0.002994	11.8	0.7327	0.1828	0.0845
B	101	12.28	193.3	0.02526	0.54	0.7844	0.1768	0.0388
C	92	12.28	187.9	0.1349	0.12	0.7873	0.2056	0.0071
D	84	12.27	201.0	0.6769	0.034	0.7615	0.2385	0

errors described hereafter. The grid system finally obtained in this calculation is shown in Fig. 5. To reduce the statistical errors, the number of sample particles in each cell was kept at the order of 10^2 in general, which typically required 10^7 sample particles in the entire calculation region.

The calculated distribution of the total number density is shown in Fig. 6 for each flight case with an AOA of 20 deg. As the freestream density increases along with the decrease of the flight altitude, the shape of the bow shock ahead of the capsule becomes more and more clear and the shock standoff distance decreases. The aerodynamic force acting on the capsule is determined when an ensemble average is taken of the kinetic momentum transferred to the capsule from samples hitting against the surface. The aerodynamic coefficients are then calculated by Eqs. (1) and (2). To obtain the final solution after the calculation convergence, the ensemble average is taken over 5000 steps with a sampling interval of twice the mean free time, and the standard deviation was defined as the statistical error. In Fig. 7, the aerodynamic coefficients obtained for an AOA of 20 deg are plotted with error bars against Knudsen number. In Fig. 8, C_m calculated with $X_c = 0.13$ m for each Knudsen number is plotted as a function of the AOA.

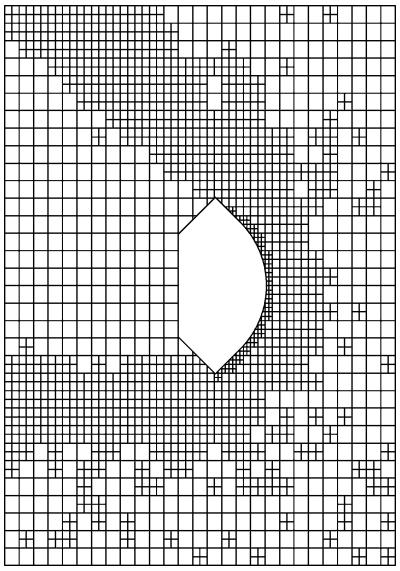

Fig. 5 Solution-adaptive grid based on local-Knudsen-number criteria, on symmetric plane altitude, 92 km and AOA, 20 deg.

In Fig. 7, the aerodynamic coefficients obtained by the collisionless DSMC calculation are also plotted at $Kn = 100$ as a matter of convenience. These coefficients are in excellent agreement with those obtained by the geometric analysis of the free-molecular flow, which are shown in Fig. 7 as the straight line at the free-molecular limit ($Kn > 10^2$). Although the flow with $Kn > 10$ is, in general, regarded to be a free-molecular flow, C_N and C_m calculated with $Kn = 11.8$ (case A in Table 2) do not agree with those of the free-molecular flow. This is because an increase in density in the vicinity of the surface, as seen in Fig. 6a, decreases the probability for molecules in the freestream to reach the capsule surface without collision. In reality, the number density closely ahead of the capsule is on the order of 10^{19}, which yields the local Knudsen number of approximately 0.3. This suggests that the Knudsen number based on the freestream conditions is only a guideline of the flow physics and that the local Knudsen number is a much better indicator of whether the flow is transitional or free molecular.

From the results shown in Figs. 7 and 8, note that the pitching stability decreases, or C_m increases, as Knudsen number increases. This is a general trend in this type of capsules. With regard to the

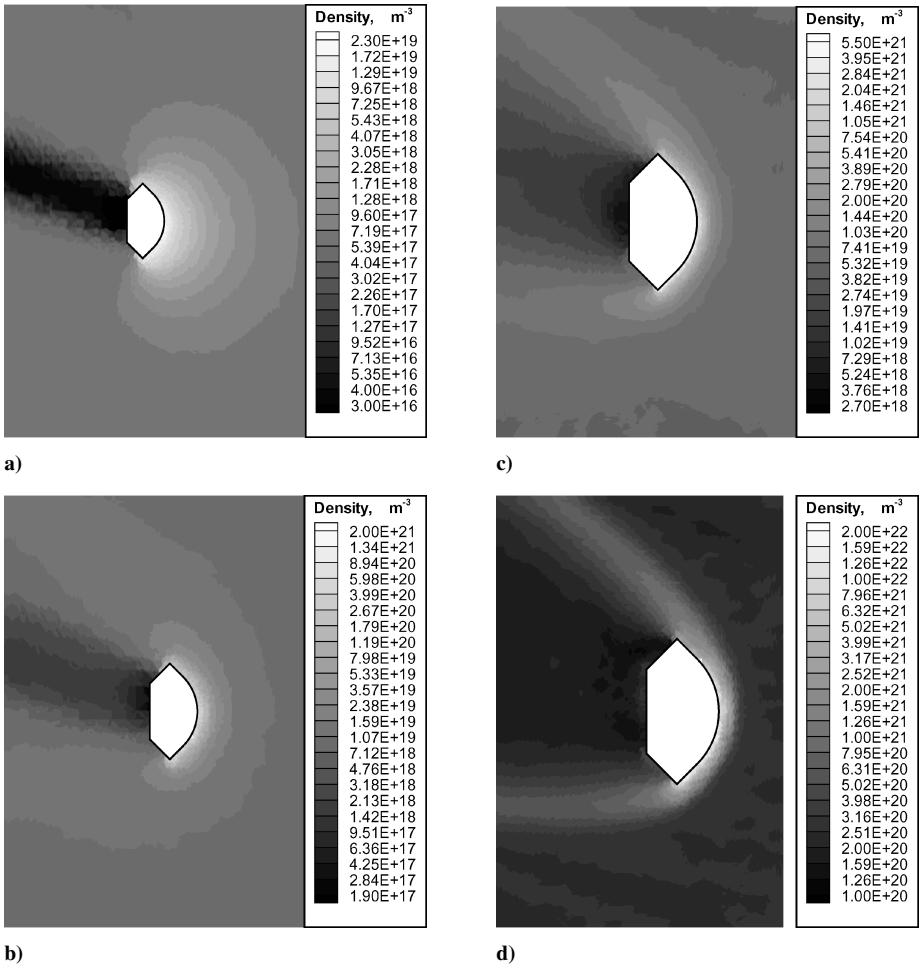

Fig. 6 Number density distribution calculated for AOA of 20 deg for altitudes of a) 120, b) 101, c) 92, and d) 84 km.

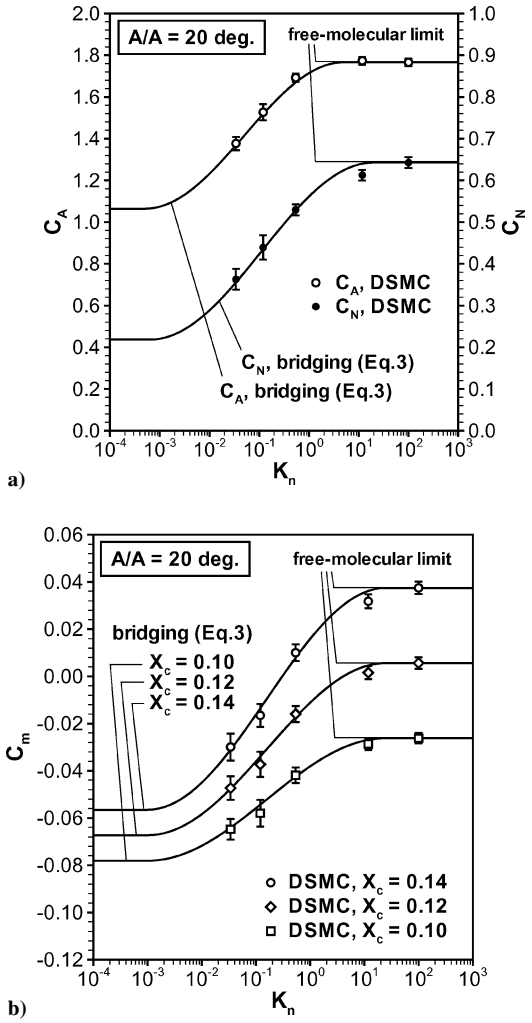

Fig. 7 DSMC aerodynamic coefficients and bridged coefficients by Eq. (3) for an AOA of 20 deg: a) axial and normal force coefficient and b) pitching moment coefficient.

MUSES-C capsule, it is necessary to make X_c less than 0.12 m if the static stability about the pitching motion should be maintained over the entire low-density flight regime.

Overall Aerodynamic Coefficients

To obtain the overall aerodynamic coefficients in the hypersonic flight regime, the aerodynamic coefficients in the continuum flow were calculated by the modified Newton method. The overall coefficients are defined by an empirical bridging formula by the use of these continuum coefficients, the transitional coefficients obtained by the DSMC analysis, and the free-molecular coefficients. In this study, the widely used sin-squared function is introduced:

$$C = C_{\text{cnt}} + (C_{\text{FM}} - C_{\text{cnt}}) \sin^2 \phi \tag{3}$$

where C is C_A, C_N, or C_m; the subscripts cnt and FM stand for the continuum and free-molecular coefficient, respectively; and

$$\phi = \begin{cases} 0 & \text{if} \quad Kn < 10^{-a/b} \\ \pi/2 & \text{if} \quad 10^{(1-2a)/2b} < Kn \\ \pi(a + b \log_{10} Kn) & \text{otherwise} \end{cases} \tag{4}$$

where a and b are adjusting parameters that are set to be $\frac{3}{8}$ and $\frac{1}{8}$, respectively, in general applications. In this study, the most appropriate a and b were determined by the least-squares method, by the use of the transitional coefficients obtained by the DSMC analysis. Here, a and b are assumed to be independent of the AOA. The

Table 3 Adjusting parameters in Eq. (4)

Coefficient	a	b
C_A	0.412	0.125
C_N	0.356	0.111
C_m	0.341	0.114

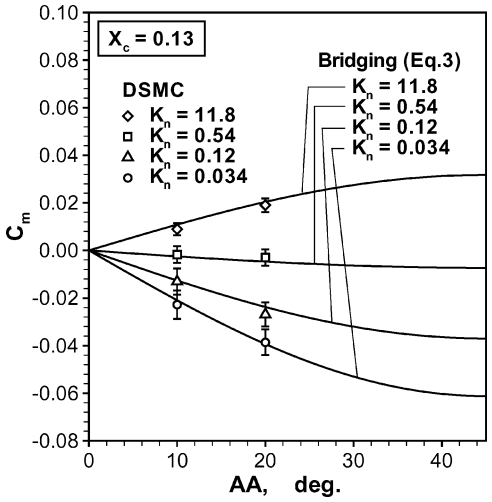

Fig. 8 Variation of pitching moment coefficient against AOA, X_c = 0.13 m.

pairs of a and b determined individually for C_A, C_N, and C_m are summarized in Table 3. To demonstrate the bridging formula, the overall aerodynamic coefficients are plotted in Figs. 7 and 8 as solid curves. Errors in the bridging coefficients compared with the DSMC results remain within ± 0.04 for C_N and C_A, and within ± 0.006 for C_m.

In the last part of this section, the property and accuracy of the aerodynamic coefficients just obtained, especially that of C_m, are discussed. It is necessary for C_m to be conservative to assess the pitching stability. The pitching instability is the most significant in the free-molecular flow, so that the most conservative values are given to the free-molecular C_m by using $\gamma = 1.0$. Neglect of the thermal velocity of molecules scattered on the capsule surface also results in a conservative estimation of C_m because a decrease of the reflected velocity is essentially equivalent to an increase in γ. For these reasons, it can be concluded that C_m in the free-molecular flow is to be determined as conservatively as possible. The transitional coefficients obtained by the DSMC analysis are also conservative because they are also determined with $\gamma = 1.0$.

Because uncertainties remain in nonequilibrium thermal relaxation and chemical kinetics in low-density flows, we examine how such uncertainties influence the aerodynamic coefficient. With regard to the cases A–C (Table 2) in which the pitching instability may occur, another DSMC calculation was made under the assumption of a thermally and chemically frozen flow. The results show that neglect of the thermal relaxation and chemical reactions increases the temperature in the shock layer. However, an increase in the temperature decreases the density accordingly. These two effects cancel each other in the pressure distribution for the capsule geometry under consideration. As a result, a slight increase of C_m, which was typically 3–5%, was only observed in the frozen flow as Knudsen number decreased; However, such an increase of C_m is within the statistical error, or the standard deviation of C_m obtained for reacting flows. In conclusion, the pitching moment coefficient defined by Eq. (3) gives the most conservative value and has statistical errors within the standard deviation.

Analysis of Capsule Dynamics

The six-degree-of-freedom dynamics of the MUSES-C capsule is numerically analyzed in the hypersonic flight regime along the

Table 4 Initial reentry conditions of MUSES-C capsule

Parameter	Value
Geometric altitude,[a] km	204.6
Geometric latitude, deg	−28.22
Geometric longitude, deg	126.64
Relative velocity, km/s	11.96
Flight-path angle, deg	−12.85
Flight azimuthal angle, deg	114.99

[a]Measured in the geodetic reference system 1980 (GRS80).

Table 5 Mass property of MUSES-C capsule

Parameter	Value
Mass, kg	16.5
C.G., m	
X_c	0.10–0.14
Y_c, Z_c	0.0
Moment of inertia, kg · m^2	
I_{xx}	0.221
I_{yy}	0.146
I_{zz}	0.136

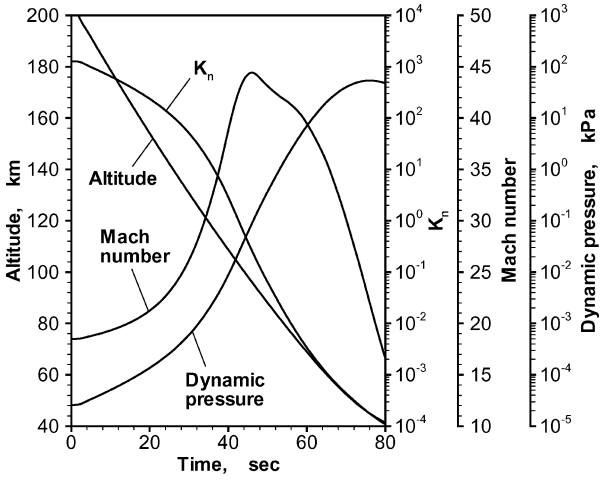

Fig. 9 Profile of flight environments along reentry trajectory, X_c = 0.10 m.

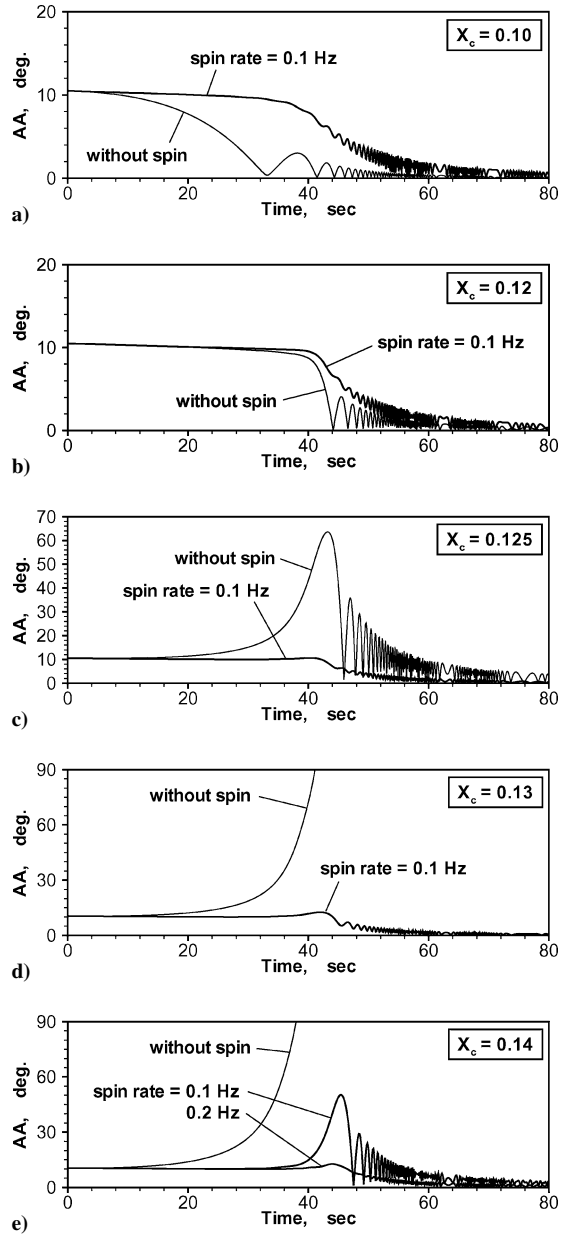

Fig. 10 Evolution of AOA along reentry trajectory: X_c = a) 0.10, b) 0.12, c) 0.125, d) 0.13, and e) 0.14 m.

reentry trajectory, from the free-molecular to continuum flow environments, with the overall aerodynamic coefficient defined by Eq. (3). The initial reentry conditions and the mass property of the capsule are summarized in Tables 4 and 5, respectively. The six equations of motion are integrated in time by the fourth-order Runge–Kutta method. The position of the c.g., or X_c defined in Fig. 1, is changed from 0.10 to 0.14 m to see the sensitivity of the pitching stability to X_c. The geodetic reference system 1980 (GRS80) is used to represent the surface of Earth. On the other hand, the NASA Marshall Space Flight Center (MSFC) global reference atmosphere model 1995 version (GRAM95)[20] is used without taking into account the dispersion in local winds and atmospheric densities.

For the sake of a conservative analysis about the pitching motion, the initial offset of the flight-path angle was assumed to be +10 deg. In reality, the initial offset is expected to be much smaller than 10 deg because the MUSES-C is designed to control the pointing direction of the capsule accurately in the reentry operation. Initial nutation is neglected, and the roll damping coefficient is assumed to be $C_{lp} = -0.01$, according to Ref. 3. The initial spin about the capsule axis was given at the frequency of 0–0.5 Hz to examine the efficacy of spin stabilization.

Time evolution of the flight altitude, the Mach number, the Knudsen number, and the dynamic pressure, are plotted in Fig. 9. Here, time is measured from the initial state defined in Table 4. Profiles of these quantities were found to be insensitive to X_c, and so only those for $X_c = 0.10$ m are presented. Numerical simulations were terminated at 80 s after the reentry, where the Mach number drops to approximately 15, because of the accuracy of the aerodynamic coefficients determined by the modified Newtonian method for the continuum flow is considered to decrease in the subsequent flight environments. When the AOA exceeded 90 deg during the calculation, the capsule was regarded as tumbling and the simulation was terminated.

Evolution of the AOA is shown in Fig. 10 for several values of X_c. Because C_m is always zero or negative, regardless of the AOA and Kn for $X_c \leq 0.12$ m, as seen in Fig. 7, the AOA is found to be attenuated regardless of the spin frequency for $X_c \leq 0.12$ m. On the other hand, unless the initial spin is given to the capsule, the AOA increases with time for $X_c > 0.12$ m, and the capsule finally tumbles for $X_c > 0.13$ m. However, in every case, the pitching stability can be achieved in hypersonic flight if the initial spin is provided at an appropriate frequency. The aerodynamic heating, which is significant from 55 to 80 s after reentry, may require the AOA to be less than 10 deg during this period to avoid an anomalous heating

distribution to the capsule surface. To actualize this, the minimum spin frequency is considered to be 0.1 Hz for $X_c \leq 0.13$ m and 0.2 Hz for $X_c \leq 0.14$ m.

The actual value of X_c is expected to lie between 0.11 and 0.13 m. Given the statistical errors in C_m, the conceivable values of C_m for X_c between 0.11 and 0.13 m do not exceed the nominal value for $X_c = 0.14$ m, as understood from Fig. 7b. For these reasons, it is concluded that the pitching motion of the MUSES-C capsule can be stabilized in the early phase of reentry by initiating the spin at a frequency of 0.2 Hz at least.

Summary

A systematic numerical procedure for assessment of the attitude stability of reentry capsules has been developed and applied practically to the MUSES-C asteroid sample return capsule. The aerodynamic coefficients of the capsule are computed for the free-molecular flow by geometric analysis, for the transitional flow by DSMC analysis, and for the continuum flow by the modified Newton method. The overall aerodynamic coefficients are defined by an empirical bridging formula by the use of the free-molecular, transitional, and continuum coefficients calculated in the paper.

The calculated coefficients show that the static stability about the pitching motion is degraded as the Knudsen number increases, depending strongly on the accommodation factor of the capsule surface. To obtain the conservative coefficients appropriate for assessment of the pitching stability, the fully diffusive surface model should be used. Uncertainties in the thermal relaxation and the chemical reaction are found to have only minor influences on the aerodynamic coefficients in the transitional flows in which the pitching instability becomes a serious problem.

The pitching stability of the MUSES-C capsule was examined by simulation of the six-degree-of-freedom dynamics of the capsule along the reentry trajectory, by the use of the overall aerodynamic coefficient. The results show that, unless the initial spin around the capsule axis is provided, it is possible for the capsule to lose the pitching stability during reentry if the c.g. is located beyond a 0.12-m distance behind the capsule forefront and, likewise, to tumble if it is located beyond a 0.13-m distance. However, such instability can be safely eliminated by initiating the spin around the capsule axis at a frequency of at least 0.2 Hz.

References

[1]Wilmoth, R. G., Mitcheltree, R. A., and Moss, J. N., "Low-Density Aerodynamics of the Stardust Sample Return Capsule," *Journal of Spacecraft and Rockets,* Vol. 36, No. 3, 1999, pp. 436–441.

[2]Inatani, Y., and Ishii, N., "Design Overview of an Asteroid Sample Return Capsule," *Aerodynamics, Thermophysics, Thermal Protection, Flight System Analysis and Design of Asteroid Sample Return Capsule*, Rept. SP 17, Inst. of Space and Astronautical Science, Sagamihara, Japan, 2003, pp. 1–15.

[3]Hiraki, K., and Inatani, Y., "The Aerodynamic Data Base for Asteroid Sample Return Capsule," *Aerodynamics, Thermophysics, Thermal Protection, Flight System Analysis and Design of Asteroid Sample Return Capsule*, Rept. SP 17, Inst. of Space and Astronautical Science, Sagamihara, Japan, 2003, pp. 345–363.

[4]Fujita, K., Inatani, Y., Hiraki, K., and Abe, T., "Rarefied Aerodynamics of MUSES-C Sample Return Capsule," *Aerodynamics, Thermophysics, Thermal Protection, Flight System Analysis and Design of Asteroid Sample Return Capsule*, Rept. SP 17, Inst. of Space and Astronautical Science, Sagamihara, Japan, 2003, pp. 333–344.

[5]Bird, G. A., "Perception of Numerical Methods in Rarefied Gas Dynamics," *Rarefied Gas Dynamics,* edited by E. P. Muntz, D. P. Weaver, and D. H. Campbell, Vol. 118, Progress in Astronautics and Aeronautics, AIAA, Washington, DC, 1989, pp. 221–226.

[6]Bird, G. A., "Monte Carlo Simulation in an Engineering Context," *Rarefied Gas Dynamics,* edited by S. S. Fisher, Vol. 74, Pt. 1, Progress in Astronautics and Aeronautics, AIAA, New York, 1981, pp. 239–255.

[7]Nanbu, K., "Variable Hard-Sphere Model for Gas Mixture," *Journal of the Physical Society of Japan,* Vol. 59, No. 12, 1990, pp. 4331–4333.

[8]Capitelli, M., Gorse, C., Longo, S., and Giordano, D., "Collision Integrals of High-Temperature Air Species," *Journal of Thermophysics and Heat Transfer,* Vol. 14, No. 2, 2000, pp. 259–268.

[9]Boyd, I. D., "Analysis of Rotational Nonequilibrium in Standing Shock Waves of Nitrogen," *AIAA Journal,* Vol. 28, No. 1, 1990, pp. 1997–1999.

[10]Parker, J. G., "Rotational and Vibrational Relaxation in Diatomic Gases," *Physics of Fluids,* Vol. 2, No. 4, 1959, pp. 449–462.

[11]Lordi, J. A., and Mates, R. E., "Rotational Relaxation in Nopolar Diatomic Gases," *Physics of Fluids,* Vol. 13, No. 2, 1970, pp. 291–308.

[12]Fujita, K., and Abe, T., "State-to-State Nonequilibrium Rotational Kinetics of Nitrogen Behind a Strong Shock Wave," AIAA Paper 2002-3217, June 2002.

[13]Fujita, K., and Abe, T., "Coupled Rotation–Vibration–Dissociation Kinetics of Nitrogen Using QCT Models," AIAA Paper 2003-3779, June 2003.

[14]Park, C., "Review of Chemical–Kinetic Problems of Future NASA Missions, I: Earth Entries," *Journal of Thermophysics and Heat Transfer,* Vol. 7, No. 3, 1993, pp. 385–398.

[15]Borgnakke, C., and Larsen, P. S., "Statistical Collision Model for Monte Carlo Simulation of Polyatomic Gas Mixture," *Journal of Computational Physics,* Vol. 18, 1975, pp. 405–420.

[16]Bird, G. A., "Simulation of Multi-dimensional and Chemically Reacting Flows," *Rarefied Gas Dynamics,* Vol. 1, Atomic Energy Commission (CEA), Paris, 1979, pp. 365–388.

[17]Boyd, I. D., "Rotational–Translational Energy Transfer in Rarefied Nonequilibrium Flows," *Physics of Fluids A,* Vol. 2, No. 3, 1990, pp. 447–452.

[18]Bird, G. A., "Application of the Direct Simulation Monte Carlo Method to the Full Shuttle Geometry," AIAA Paper 90-1692, June 1990.

[19]Bird, G. A., *Molecular Gas Dynamics and the Direct Simulation of Gas Flows,* Clarendon, Oxford, 1994, Chaps. 1, 14, 16.

[20]Justus, C. G., Jeffries, W. R., III, Yung, S. P., and Johnson, D. L., "The NASA/MSFC Global Reference Atmosphere Model-1995 Version (GRAM-95)," NASA TM-4715, Aug. 1995.

W. Williamson
Associate Editor